

AN ELECTROSTATIC FUSION COLLIDER FOR INTERSTELLAR PROPULSION

G.P. Jackson^{2,†}, G.E. Bittlingmaier¹, A.S. Lee¹

¹Beam Alpha Incorporated, West Chicago, IL, USA

²Hbar Technologies, LLC, West Chicago, IL, USA

Abstract

In order to reach the nearest star Proxima Centauri within a century, a distance of 4.224 ly from our solar system, the average spacecraft velocity needs to be 4.2% of the speed of light. Therefore, according to the rocket equation, the weighted average exhaust velocity needs to be over 1% of the speed of light for reasonable ratios of dry mass to fuel mass. The fusion reactor architecture presented herein consists of an electrostatic charged particle trap that brings two ion beams into collision with equal and opposite momentum. The two fusion channels under consideration for interstellar missions are p/Li7 and He3/He3, utilizing an array of low mass electrodes that minimize interactions with fusion daughters escaping from the collision point and focused to generate thrust. A terrestrial prototype colliding beam accelerator has been built to determine the viability of achieving collider luminosities commensurate with the requirements of this application. A novel architecture overcomes past Coulomb scattering limitations. Reactor and propulsion system design parameters are presented in this paper along with fabrication and testing status.

PROPELLION

The fusion reactor architecture used in the proposed propulsion system [1] consists of an electrostatic charged particle trap [2-4] that brings two ion beams into collision with equal and opposite momentum. For the purposes of this paper only deceleration at Proxima Centauri is addressed.

Assume a fuel mass of M_{fuel} before deceleration. After expending all of the fuel the spacecraft mass is represented as M_{dry} . Let N be the number of mass stream species, each with a fraction of the total exhaust mass α_i and exhaust velocity with respect to the spacecraft v_i . The change in spacecraft velocity ΔV is

$$\Delta V = \sum_{i=1}^N \alpha_i v_i \ln(1 + M_{\text{fuel}}/M_{\text{dry}}) \quad , \quad (1)$$

where

$$1 = \sum_{i=1}^N \alpha_i \quad . \quad (2)$$

Figure 1 shows the relationship of Eq. (1) as a function of the mass-weighted average exhaust velocity. Observe the diminishing returns upon fuel-to-dry mass ratio approaching 20:1, as the ratio between spacecraft and exhaust velocity levels out. In order to decelerate a spacecraft from at least one percent of the speed of light, the fusion daughter particle velocities escaping the propulsion system must also be at least one percent of lightspeed. Hence direct fusion daughter emission from the collider is required.

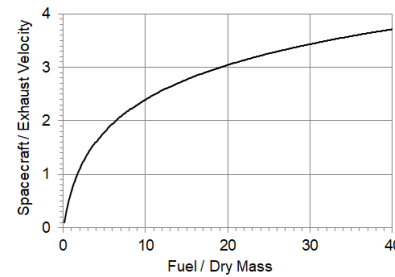


Figure 1: Rocket equation prediction of change in spacecraft velocity relative to the weighted average exhaust velocity as a function of ratio of fuel to dry mass.

The proposed architecture to accomplish this task is illustrated in Fig. 2. Assuming a 100-year transit time, a constant 10-year acceleration, and a 10-year deceleration burn, the peak spacecraft velocity during the 80-year coast period is 0.042c. The peak acceleration of the spacecraft is 0.029 m/s². This is approximately 0.3% of gravity at the Earth surface, allowing the use of fragile spacecraft components such as electrodes composed of thin wires similar to the vacuum ion gauge pictured to the right.

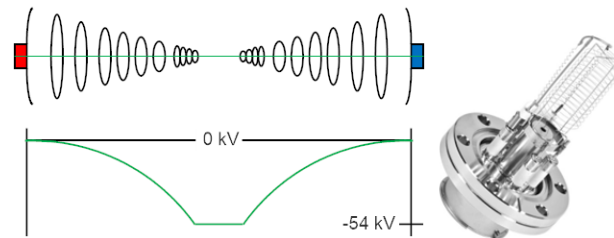


Figure 2: On the left side, illustration of the electrostatic electrode array of the fusion collider (top) and the axial potential (bottom). The right side is a picture of a standard vacuum ion gauge.

This collider architecture enables direct fusion daughter escape. Utilizing an electrostatic nozzle¹, the escaping particles are focused into a coherent exhaust stream while maintaining their initial kinetic energy.

FUSION CROSS SECTIONS

One nuclear fusion fuel combination under consideration is helium-3 on helium-3. As graphed in Fig. 3, this reaction has a peak cross section of 0.115 barns. In a symmetric collider this peak corresponds to a beam kinetic energy of 4 MeV. For axial confinement the depth of the axial potential must therefore be at least 2 MV. Operating the electrostatic collider at a axial potential depth of 1 MV is possible with only a 20% reduction in cross section. A 40% drop in cross section allows operation at 500 kV.

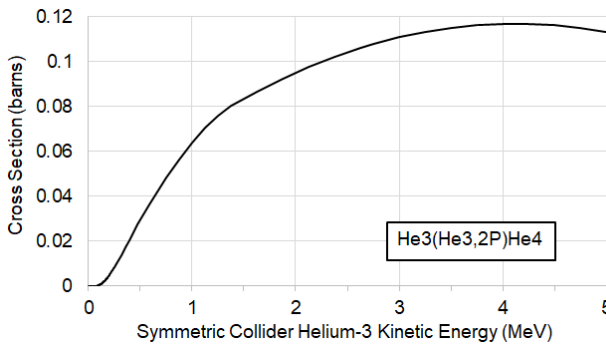
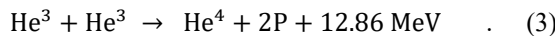


Figure 3: Helium-3 on helium-3 cross section in a symmetric collider as a function of beam kinetic energy.

The nuclear fusion reaction for helium-3 is



wherein the three fusion daughters share the reaction kinetic energy of 12.86 MeV consistent with conservation of momentum. Each daughter has an energy range between zero and 4.3 MeV for the alpha particle (He^4) and 10.71 MeV for the protons (P). These maxima increase with increasing collision kinetic energies between the helium-3 nuclei.

The weighted average exhaust velocity of Eq. (1), averaged over all configurations, is approximately 0.052c. At a helium-3 beam energy of 1 MeV the weighted average exhaust velocity increases to 0.059c. This corresponds to a minimum fuel-to-dry mass ratio of 1.42.

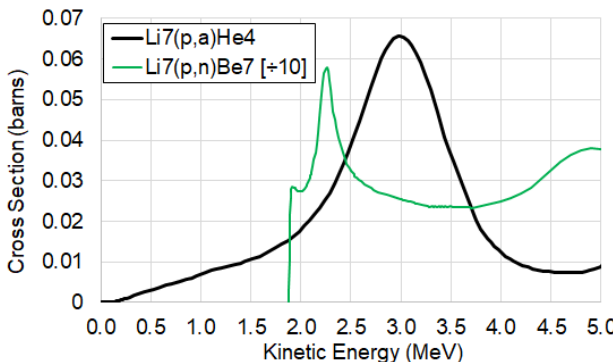
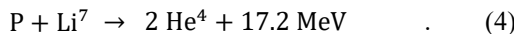


Figure 4: Cross sections for an incident proton on a stationary lithium-7 target (black). Superimposed is a secondary fusion reaction (green), suppressed by a factor of ten to fit on the same scale, with a threshold of 1.93 MeV.

Another nuclear fusion fuel combination under consideration is protons and lithium-7. The measured fixed target cross section spectrum of this reaction, as a function of incident proton kinetic energy, is graphed in Fig.4. The energetics of the reaction are



In this fixed target case there is a maximum proton kinetic energy of 1.93 MeV, where threshold is achieved for the much higher cross section reaction producing beryllium-7. Because this reaction is at threshold, the fusion daughters are emitted with zero kinetic energy, and hence produces zero thrust. When both beams have equal momentum in a symmetric collider the proton and lithium-7

kinetic energies are 1.475 MeV and 0.212 MeV, respectively. This corresponds to a weighted average exhaust velocity of 0.071c, and a fuel-to-dry mass ratio of 0.91.

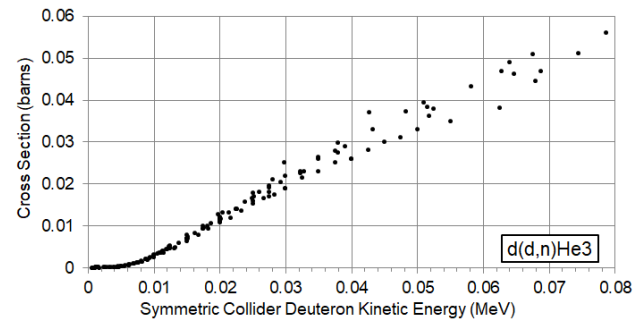


Figure 5: Low energy cross section for DD neutron production. The peak DD fusion cross section is 0.1 barns.

A terrestrial prototype colliding beam accelerator [5] has been built to determine the viability of achieving collider luminosities commensurate with the requirements of this application. In order to monitor luminosity on a real-time basis, a low energy fusion reaction was desired with plentiful and inexpensive fuel that produces neutrons. DD fusion is that reaction, emanating neutrons with a kinetic energy of approximately 2.5 MeV. A graph of the DD fusion cross section for neutron production, as a function of deuteron beam energy, is graphed in Fig. 5.

LUMINOSITY

The rate of fusion reactions R within the collider is determined by the product of the fusion cross section σ_{xs} and a quantity called luminosity L

$$R = L \sigma_{xs} \quad , \quad (5)$$

where the luminosity is defined by the equation

$$L = \frac{I^2 \beta^*}{2 v^* \sigma^{*2}}$$

This form of the equation assumes DC continuous beams with identical beam current I, round radial beam size σ^* , velocities v^* , and a collision point beta function value β^* .

For a 100 kg dry mass and helium-3 fusion, a luminosity of $3.9 \times 10^{44} \text{ cm}^{-2} \text{ s}^{-1}$ is required. This corresponds to a fusion rate of 6.45 mole per day at the peak cross of 0.115 barns. In June 2020 the SuperKEKB collider in Japan announced a record luminosity of $2.2 \times 10^{34} \text{ cm}^{-2} \text{ s}^{-1}$. The CERN LHC has been steadily increasing in luminosity via a series of accelerator upgrades, expected to reach $7.5 \times 10^{34} \text{ cm}^{-2} \text{ s}^{-1}$. For historical perspective, the Tevatron Collider had a design luminosity of $1.0 \times 10^{30} \text{ cm}^{-2} \text{ s}^{-1}$ in 1988 and ended operations at a luminosity 500 times greater by 2011 with a peak luminosity of $4.5 \times 10^{32} \text{ cm}^{-2} \text{ s}^{-1}$. The accelerator physics community has consistently demonstrated the ability to achieve collider performance levels far exceeding those initially designed.

Studying the terrestrial prototype, low luminosities are anticipated during initial commissioning. For a luminosity of $1 \times 10^{27} \text{ cm}^{-2} \text{ s}^{-1}$ a cross section of 0.3 barns produces a neutron production rate of 30 Hz. With an overall detection

efficiency of 3%, a counting rate of 1 Hz is achievable. While such low luminosities are probable in the early days of collider operations, it is anticipated that luminosities several orders of magnitude greater are achievable.

The radial lattice formed by the axial potential in Fig. 2 is stable within a limited kinetic energy window. In the case of deuterons in the terrestrial prototype collider, the bounce period (or revolution period for those more comfortable with circular colliders) increases with beam energy due to deeper axial trajectories into the quadratic potentials on either axial side of the collider. Calculation results of the bounce period within the stable energy window are graphed in Fig. 6.

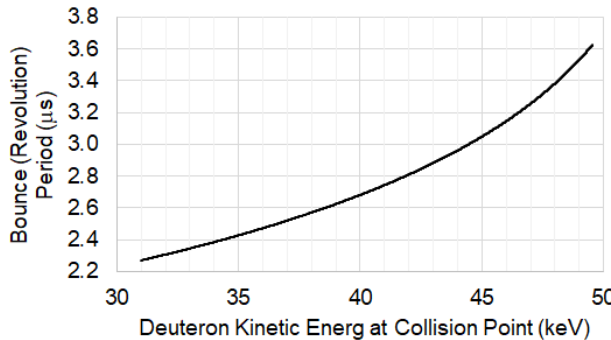


Figure 6: Bounce (revolution) period for deuterons in the terrestrial prototype collider.

The beta-star β^* (presented in units of time instead of distance) is calculated again within the energy window of the terrestrial prototype collider filled with deuterons. Graphed in Fig. 7, there is a broad energy region of beta-star between 2 and 0.5 μ s between two divergent end regions. These graphs are used to estimate luminosity for a given beam energy and current.

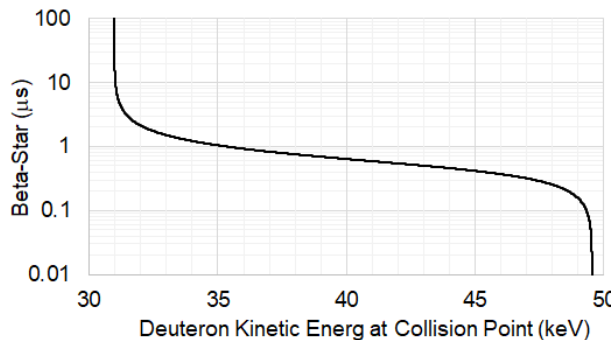


Figure 7: Calculated beta-star for deuterons in the terrestrial prototype collider.

COULOMB SCATTERING

A common criticism of this colliding beam approach to nuclear fusion is that the beam size σ^* increases very quickly due to large-angle Coulomb scattering. In traditional fusion machines the plasma is excited to high temperatures with an external power source. This corresponds to an energy of 5-10 keV per nucleus. Because of this initial investment, a given fraction of fuel nuclei must undergo fusion in order to generate more energy than is deposited into the plasma. Therefore, preservation of nuclei

is paramount. In the case of this proposed electrostatic collider architecture, the initial energy investment is under 100 eV, two orders of magnitude smaller.

Assume a particular fuel nucleus undergoes a significant Coulomb scattering deflection near the central collision region. The electrodes in the collider architecture illustrated in Fig. 2 have radial apertures that grow linearly with distance from the collider center. Unlike traditional circular synchrotrons with apertures limited by magnet gaps, this geometry allows highly divergent particles to generate luminosity.

Once a fuel nucleus approaches the radial aperture of the collider, it is beneficial to remove it at a point where its kinetic energy is nearly zero. This location is out near the extreme axial bounce region where the nuclei stop and reverse course. A simple annular electrostatic septum is being designed to remove such particles, reminiscent of an annular Faraday cup.

The above procedure thus calls for continuous injection of fuel. Quickly pulsing the voltage on the outer electrodes, over a period of nanoseconds compared to the microsecond bounce period graphed in Fig. 6, enables the injection of short bursts of fuel current wherein the loss of stored beam is minimized and a constant beam current is maintained.

CONCLUSION

In order to reach the nearest star within a century with an orbiting scientific probe, a propulsion system based on colliding beam nuclear fusion has been proposed. Two candidate fuels are under consideration. The achievement of sufficient luminosity to enable such missions represents a challenge to the accelerator physics community. A terrestrial prototype collider has been fabricated to study high luminosity in such an accelerator architecture. Mitigation of large-angle elastic Coulomb scattering effects are also a significant subject of research.

REFERENCES

- [1] G. P. Jackson and G. E. Bittlingmaier, "Fusion Propulsion Constraints Required by Robust Exoplanet Exploration," *Nuclear Science and Technology Open Research*, vol. 3, p. 9, Feb. 2025. [doi:10.12688/nuclscitechnotopenres.17640.1](https://doi.org/10.12688/nuclscitechnotopenres.17640.1)
- [2] C. A. Ordóñez and D. L. Weathers, "Two-species mixing in a nested Penning trap for antihydrogen trapping," *Phys. Plasma*, vol. 15, no. 8, p. 083504, Aug. 2008. [doi:10.1080/00295450.2021.1997057](https://doi.org/10.1080/00295450.2021.1997057)
- [3] S. P. Møller, "ELISA, and electrostatic storage ring for atomic physics," *Nucl. Instrum. Methods Phys. Res. A*, vol. 394, no. 3, pp. 281–286, Jul. 1997. [doi:10.1016/s0168-9002\(97\)00673-6](https://doi.org/10.1016/s0168-9002(97)00673-6)
- [4] G. P. Jackson, "Antimatter-Based Propulsion for Exoplanet Exploration," *Nucl. Technol.*, vol. 208, no. sup1, pp. S107–S112, Jan. 2022. [doi:10.1080/00295450.2021.1997057](https://doi.org/10.1080/00295450.2021.1997057)
- [5] G.E. Bittlingmaier, G.P. Jackson, and A.S. Lee, "Instrumentation for a Prototype Fusion Propulsion System", presented at NAPAC'25, Sacramento, CA, Aug. 2025, paper MOP051, this conference.